



OPEN

Lower limb muscle synergies during deceleration at different change of direction angles

Hongxiang Zhang^{1,4}, Haoyang Wang^{1,4}, Huan Long²✉ & Xinyu Zhang³

Change of direction is a core technical action in many competitive sports such as football and basketball, and it plays a crucial role in athletes' performance. Deceleration, which is the foundation of changing direction, has been proven to be a key element in athletes' rapid directional changes. This study collected electromyographic signals during the deceleration phase of a 45° and 90° left change of direction in 16 male college football players, and analyzed their muscle synergies using non-negative matrix factorization to extract key indicators such as the number of synergy modules and muscle weights. The study found that two stable muscle synergy modules could be extracted during the deceleration phase of both 45° and 90° changes of direction. synergy module 1 was dominated by the biceps femoris, semitendinosus, and vastus lateralis; synergy module 2 was dominated by the rectus femoris, vastus medialis, and tibialis anterior. When the change of direction angle increased from 45° to 90°, the weight of the tibialis anterior in synergy module 1 significantly decreased ($P=0.029$), and the weights of the vastus lateralis and biceps femoris in synergy module 2 significantly increased ($P=0.014$ and $P=0.049$). Other synergy parameters (such as the time to peak activation, the degree of synergy module activation, the proportion of obvious activation duration, overall activation degree, and co-activation duration) showed no significant differences ($P > 0.05$). This indicates that during deceleration in both 45° and 90° changes of direction, there are two stable muscle synergy modules. synergy module 1 is dominated by the biceps femoris, semitendinosus, and vastus lateralis, while synergy module 2 is centered around the rectus femoris, vastus medialis, and tibialis anterior. These two elements are jointly responsible for deceleration, initial direction change, and joint stability maintenance. As the change of direction angle increases, the human lower limb prioritizes enhancing knee joint stability, at the expense of some ankle joint control. Therefore, targeted training should focus on optimizing knee joint stability, strengthening the eccentric force of the hamstring muscles, and improving dynamic control of the ankle joint.

Keywords Deceleration, Muscle synergy, Neuromuscular control

Change of direction (COD) is a core technical movement in many competitive sports, such as football and basketball, and plays a crucial role in athletes' performance. It requires athletes to quickly and accurately change their direction of movement while maintaining body balance and stability at high speeds. Statistical data show that football players can change direction more than 700 times in a single match¹. Research indicates that the ability to change direction is a key indicator distinguishing elite from sub-elite athletes^{2,3}, and its quality directly determines the effectiveness of breaking through, defending, and executing tactics in a game.

Deceleration, as one of the three phases of COD (acceleration, deceleration, and re-acceleration)^{4,5}, has been proven to be the foundation of athletes' rapid COD^{6,7}. Rapid deceleration enables players to quickly transition to other movements, thereby facilitating the success of both offense and defense^{8,9}. However, there are significant differences in the deceleration strategies required for different COD angles. Larger COD angles typically require longer deceleration distances, stronger braking capabilities¹⁰, and higher levels of muscle activation¹¹. This indicates that in training, precise training should be conducted according to the characteristics of different COD angles to better meet the needs of athletes in various situations.

Current research on deceleration mainly focuses on horizontal deceleration^{12,13}, with insufficient attention to deceleration in anticipated COD scenarios. Meanwhile, studies on COD primarily analyze the entire COD

¹Wuhan Sports University, Wuhan 430070, China. ²Sports Department, North China Institute of Science and Technology, Hebei 065201, China. ³Nanjing Sport Institute, Nanjing 210000, China. ⁴Hongxiang Zhang and Haoyang Wang contributed equally to this work. ✉email: lhlh202404@163.com

phase rather than the deceleration preparation phase, which is a component of the COD^{11,13}. For instance, Falch et al.¹¹ investigated the changes in muscle activation and kinematic characteristics under different approach distances and COD angles, but their research focus was not on the neuromuscular control mechanisms during the deceleration phase. Pan et al.¹⁴ used non-negative matrix factorization (NMF) to study muscle synergies during lateral cutting movements. However, their analysis unit was the entire stance phase, without specifically focusing on the key deceleration step. These limitations in methodology and analytical perspective have led to a lack of understanding of the neuromuscular control mechanisms during the deceleration phase in anticipated COD situations, thereby restricting the scientific formulation of targeted training strategies.

Muscle synergy refers to the coordinated activation of groups of muscles, which allows the central nervous system to control movement through a smaller number of core variables rather than individual muscles^{15,16}. The coordination and stability of movement depend on the regularity of the synergy modules¹⁷. In tasks that require instantaneous coordination of multi-joint braking, such as COD deceleration, muscle synergies are also affected differently. Therefore, it is necessary to clarify the modular control characteristics of the central nervous system and the changes in lower limb muscle synergies during deceleration at different COD angles.

Based on this, this study intends to use surface electromyography (sEMG) combined with the Non-negative Matrix Factorization (NMF) method to investigate the muscle synergy characteristics during the deceleration step under different anticipated COD angles. Referring to the findings of Falch et al.¹¹, this study will primarily focus on the differences in muscle synergy patterns during the deceleration step before speed-dominant directional changes (45° and 90°). The research hypothesis is that 45° and 90° directional changes share common synergy modules during the deceleration step but exhibit significant differences in the weightings of certain muscles and their activation characteristics.

Materials and methods

Experimental participants

From April to May 2025, 16 male collegiate athletes were recruited at Wuhan Sports University (age 20.60 ± 1.05 year, height 179.60 ± 3.94 cm, body mass 76.53 ± 7.11 kg, 6–10 year training history, 3–5 sessions wk^{-1} , 120 min session $^{-1}$). All participants were right-leg dominant and had sustained no lower-limb injuries that could affect performance in the six months preceding testing.

Prior to the testing, all participants were fully informed in writing about the potential risks and safety guidelines related to the testing procedures and signed informed consent forms. Participants wore wireless surface electromyography sensors and completed the 45° and 90° COD tests. The study protocol was approved by the Ethics Committee of Wuhan Sports University (approval number: 2025101) and followed the ethical guidelines of the Helsinki Declaration.

Experimental instruments

Wireless surface electromyography was recorded with the U.S.-made Delsys Trigno™ system. Following the electrode-placement guidelines of Hermens et al.¹⁸, wireless Surface Electromyography sensors were positioned precisely on each participant. Consistent with previous work¹⁹, signals were collected from the vastus lateralis (VL), rectus femoris (RF), vastus medialis (VM), biceps femoris (BF), semitendinosus (ST), tibialis anterior (TA), and gastrocnemius lateralis (GL) at a sampling frequency of 2,000 Hz.

A three-dimensional motion capture system (SIMIMO-TION, Germany) was employed. In this study, five high-speed cameras were positioned around the COD area to record the athletes' movements during the COD process in order to identify the changes in the phases of the COD. After the test, the video data were imported into the motion capture system analysis software and filtered using a Butterworth low-pass filter with a cutoff frequency of 10 Hz²⁰.

Experimental protocol

Prior to the test, the subjects are required to complete the following preparations: First, the electromyography electrodes are attached. Then, a 5-minute jog is conducted to warm up, increase heart rate and body temperature. Subsequently, a 5-minute dynamic stretching is performed to activate the muscle groups, enhance joint mobility, and prevent sports injuries. After the warm-up, the subjects complete several practice trials at full speed to familiarize themselves with the testing procedure.

The testing method was designed in reference to the experiments conducted by Falch et al.¹¹ and Schreurs et al.²¹ (see Fig. 1). The COD test included 45° and 90° left turns, which were primarily executed by the participants' dominant foot (right foot). The specific procedure was as follows: Participants started from a standing position with their front foot 20 centimeters away from the timing gate. They first sprinted 5 meters in a straight line, then turned left, and finally sprinted another 5 meters to reach the finish line. Infrared timing gates were set at both the starting point and the finish line to measure the time taken for the COD. Each direction was tested three times, and the best trial was used for subsequent EMG analysis. Because different COD angles impose distinct muscular loads¹⁰, the order of these blocks was randomized across participants to eliminate sequence effects. To prevent fatigue, participants were given adequate rest (5 min) between each trial block. The definition of the deceleration phase in this study is based on gait definitions. Specifically, the deceleration phase is defined as a braking gait cycle occurring before the plant step¹¹, analyzing the electromyographic (EMG) indicators from the initial contact of the heel on the side opposite to the change of direction angle until the same heel contacts the ground again, covering a complete gait cycle.

Data processing

The raw EMG signals were first processed with a band-pass filter of 10–500 Hz and then full-wave rectified. The rectified signals were enveloped using a 4th -order low -pass Butterworth filter with a cutoff frequency of 10

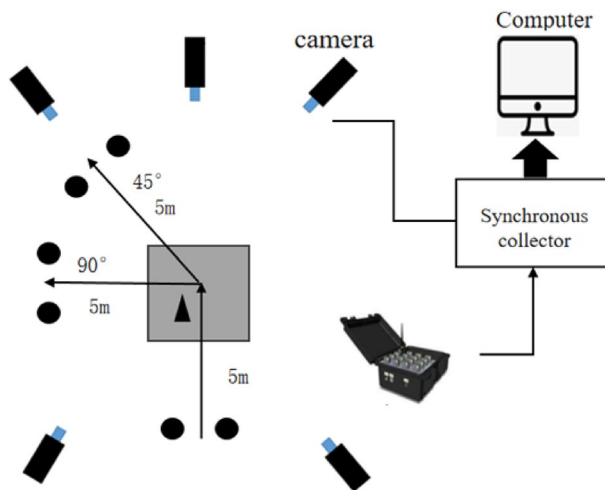


Fig. 1. Measurement setup and equipment placement.

Hz²². Referring to previous research¹⁴, the signals were normalized using their maximum values. The time axis was normalized to the range of 0–100% by linear interpolation, making signals of different lengths comparable in time²³. Surface electromyography (EMG) signals were collected from seven target muscles (VM, RF, VL, BF, ST, GL, TA) and processed to form a 7×101 -dimensional feature matrix E (where $m = 7$ represents the number of muscles and $n = 101$ is the length of the time sequence) in the aforementioned order. Subsequently, the non - negative matrix factorization algorithm²⁴ (Formula 1) was applied to decompose this matrix into a k - dimensional synergy matrix W representing muscle synergy patterns and an activation coefficient matrix H reflecting temporal activation characteristics. The feature matrix E'(Formula 2) was reconstructed through matrix multiplication (W×H) for subsequent analysis.

$$E = \sum_{i=1}^N W_i H_i + e, \quad W_i \geq 0, \quad H_i \geq 0 \quad (1)$$

$$E' = \sum_{i=1}^N W_i H_i, \quad W_i \geq 0, \quad H_i \geq 0 \quad (2)$$

Note: N is the number of muscle synergies, and e is the residual.

Subsequently, key synergy features were extracted from the original feature matrix E and its reconstructed matrix E' of muscle activation patterns. The specific analysis indicators and criteria are as follows:

- (1) Number of muscle synergies involved: The variance accounted for (VAF) analysis method was used to compare the variance and its rate of change between the reconstructed feature matrix E' and the original matrix E (Formula 3). The criterion for determining the number of synergies involved is a VAF value greater than 90%^{25–27}.

$$VAF = 1 - \frac{\sum_{i=1}^m \sum_{j=1}^n (E_{ij} - E'_{ij})^2}{\sum_{i=1}^m \sum_{j=1}^n (E_{ij})^2} \quad (3)$$

- (2) Muscle Relative Weight. The contribution of muscles is derived from the decomposition of the original matrix E, which can be used to compare the differences in muscle contributions within the same synergy for different gait COD angles²⁸.
- (3) Time to Peak Activation of Muscle Synergies. The coefficient matrix H, which is decomposed from the original matrix E, can reflect the activation intensity of each synergy. The time at which the activation intensity of each muscle synergy reaches its peak is recorded²⁶.
- (4) Activation Level of Muscle Synergies and Overall Activation Level. The coefficient matrix H can also be used to evaluate the muscle activation intensity of each synergy and the overall activation level of the synergy structure³⁰. The activation level of each muscle synergy is defined as (Formula 4):

$$E_i(\text{Activation Level}) = \frac{1}{n} \sum_{j=1}^n H_{ij} \quad (4)$$

Note: H_{ij} is the element in the i -th row and j -th column of the activation coefficient matrix H , representing the activation intensity of the i -th muscle synergy at the j -th time point. n is the length of the time sequence.

(5) Duration of Significant Activation and Co-activation of Muscle Synergies. The duration of significant activation of a muscle synergy refers to the length of time during which the activation level of a particular muscle synergy exceeds 50% of its maximum activation level. Co-activation refers to the proportion of time during which two or more muscle synergies are simultaneously in an activated state.

Statistical analysis

In this study, SPSS 21.0 software was used for statistical analysis. First, the K-means clustering algorithm was applied to cluster the synergy modules before and after the experiment. Based on this, Pearson correlation analysis (with a threshold set at $r=0.6$) was used to categorize the extracted synergy modules. Synergy modules with $r > 0.6$ were grouped together to identify types of muscle synergies³¹. In the analysis of differences before and after the experiment, since the synergy modules participated by individuals were not entirely consistent before and after the experiment, only the synergy modules that existed in both periods were selected for paired analysis. The specific methods are as follows: First, the Shapiro-Wilk test was used for normality analysis. If the data conformed to a normal distribution, paired sample t-tests were employed to compare the differences in various indicators between the two groups; if the data did not conform to a normal distribution, the Wilcoxon signed-rank test was used for comparison. The significance level for statistical analysis was set at $P < 0.05$, and differences were considered statistically significant. The datasets generated during this study are available in the Figshare repository: (DOI: <https://doi.org/10.6084/m9.figshare.30092332.v1>).

Results

Matrix decomposition results

In this study, non-negative matrix factorization was performed on the electromyographic signals of the deceleration step for 45° and 90° change of direction sprints. Although there were significant differences in the synergy weights between the two angles ($P > 0.05$), overall, two sets of synergy modules could be extracted under both COD angles (see Figs. 2 and 3). Synergy 1 was dominated by the biceps femoris, semitendinosus, and vastus lateralis, while Synergy 2 was dominated by the rectus femoris, vastus medialis, and tibialis anterior.

Matrix Decomposition Results When the Variance of Functional Activation (VFA) was greater than 90%, the number of muscle synergy modules for the deceleration steps at 45° and 90° was mostly 2. When the number of synergy modules was 3, the VFA of all individuals' synergy modules was greater than 90% (see Fig. 4). There was no significant difference in the number of synergy modules between different angles $P > 0.05$ ($P > 0.05$).

Comparison of Synergy Parameters As the COD angle increased from 45° to 90° , significant changes were observed in the muscle weightings across different synergy modules. In Synergy Module 1, the weighting of tibialis anterior (TA) significantly decreased (45° : 0.460 ± 0.252 , 90° : 0.324 ± 0.204 , $P = 0.029$). In Synergy Module 2, the weightings of both vastus lateralis (VL) and biceps femoris (BF) showed significant increases (VL: 45° 0.203 ± 0.224 , 90° 0.395 ± 0.281 , $P = 0.014$; BF: 45° 0.142 ± 0.124 , 90° 0.276 ± 0.249 , $P = 0.049$). The weightings of the remaining muscles showed no statistically significant differences between the two COD angles ($P > 0.05$) (see Table 1).

Although some muscles exhibited changes in their weights within the synergy modules across the two change of direction angles, other synergy parameters, such as the time to peak activation, Activation Level of Synergy, the proportion of Significant activation duration, the overall activation level, and the duration of co-activation, showed no significant differences ($P > 0.05$) (see Table 2).

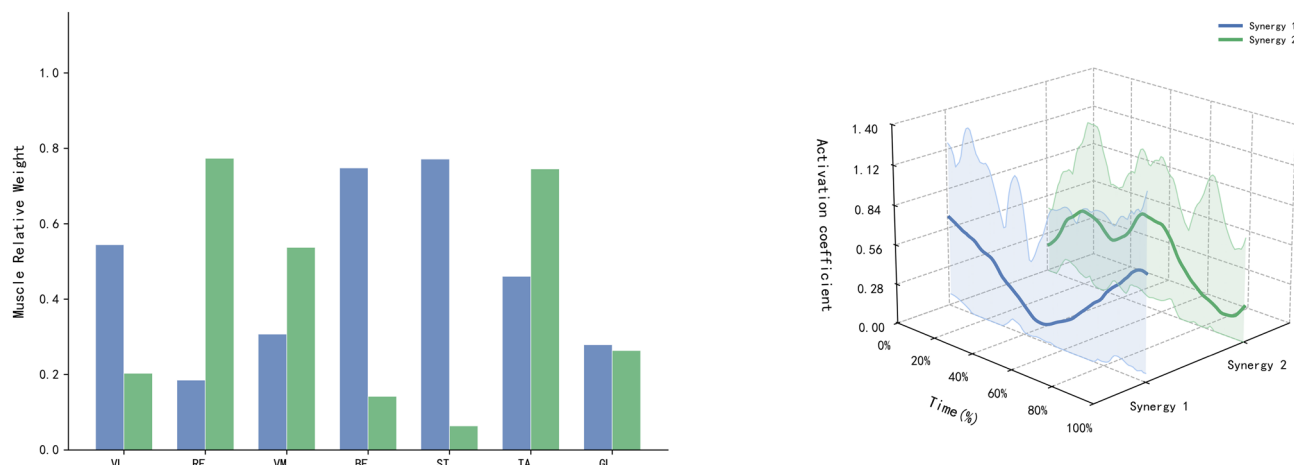


Fig. 2. Synergy matrix W and activation coefficient matrix H for the 45° Deceleration.

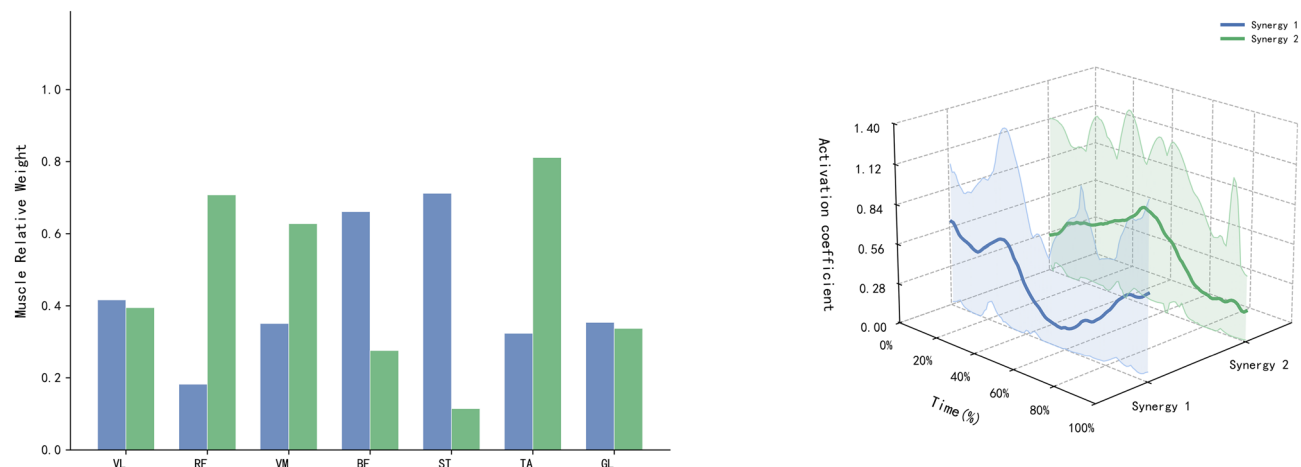


Fig. 3. Synergy matrix W and activation coefficient matrix H for the 90° Deceleration.

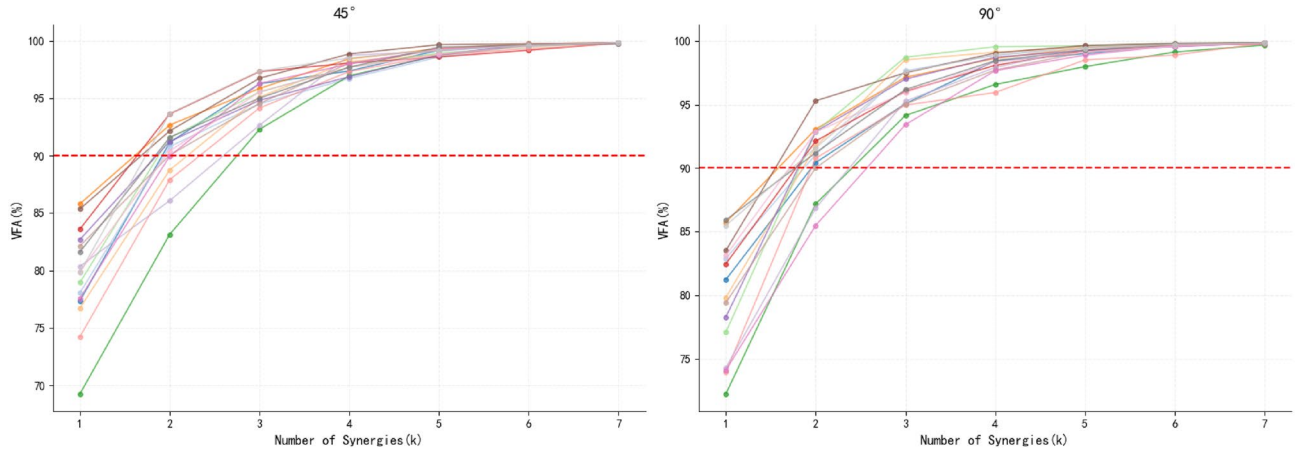


Fig. 4. Variation of VFA values with the number of synergies at different angles.

Discussion

This study found that during the deceleration phase of both 45° and 90° COD maneuvers, two distinct muscle synergy modules were consistently identified. This structural characteristic reflects the presence of a neurocontrol template in anticipatory directional changes. The modular organization suggests that the central nervous system employs predefined synergy templates, adapting to different COD demands by modulating activation timing and intensity rather than reconstructing new synergy modules to optimize motor performance, which aligns with the findings of Pan et al.¹⁴ on synergy patterns during various side-step cuttings.

Specifically, Synergy Module 1 was dominated by the biceps femoris (BF), semitendinosus (ST), and vastus lateralis (VL), while Synergy Module 2 was primarily composed of the rectus femoris (RF), vastus medialis (VM), and tibialis anterior (TA). As the COD angle increased from 45° to 90° , significant changes in muscle weightings were observed during the deceleration step. At 90° , the weighting of the tibialis anterior (TA) in Synergy Module 1 significantly decreased ($P = 0.029$). In Synergy Module 2, the weightings of the vastus lateralis (VL) and biceps femoris (BF) showed significant increases ($P = 0.014$ and $P = 0.049$). In contrast, no significant differences were found in other synergy parameters, such as time to peak activation and co-activation duration. Notably, the integration of anatomically antagonistic muscles such as the biceps femoris (BF) and vastus lateralis (VL) within the same synergy module demonstrates a distinct muscle co-activation pattern during COD maneuvers. This pattern serves as a crucial neural control strategy, closely associated with regulating joint stiffness, maintaining postural stability, and optimizing energy efficiency^{32,33}. Therefore, while this study provides evidence for understanding the efficient and stable synergy modules control strategies employed by the central nervous system during rapid deceleration in directional changes, the specific mechanisms warrant further investigation through biomechanical modeling and analysis of neural drive signals.

When the COD angle increased, corresponding adjustments were observed in the muscle synergy patterns. During 90° COD maneuvers, the demand for hip and knee joint moments surged significantly. This study found a notable reduction in the weighting of the tibialis anterior (TA) within Synergy Module 1 ($P=0.029$). This phenomenon suggests that under larger COD angles, the central nervous system may temporarily reduce resource

Synergy type	Muscle	45° (Mean±SD)	90° (Mean±SD)	Statistic	P-value	Effect size
Synergy 1	VL	0.544±0.274	0.416±0.320	1.686	0.111	0.409
	RF	0.185±0.168	0.182±0.237	-0.828 ^a	0.431	0.191 ^b
	VM	0.307±0.244	0.351±0.251	-0.719	0.483	0.174
	BF	0.748±0.207	0.661±0.252	1.146	0.269	0.278
	ST	0.771±0.125	0.712±0.260	1.035	0.316	0.251
	TA	0.460±0.252	0.324±0.204	2.398	0.029*	0.582
	GL	0.279±0.225	0.354±0.280	-0.831	0.419	0.201
Synergy 2	VL	0.203±0.224	0.395±0.281	-2.815	0.014*	0.727
	RF	0.773±0.244	0.707±0.256	0.786	0.445	0.203
	VM	0.537±0.216	0.628±0.258	-0.341 ^a	0.762	0.078 ^b
	BF	0.142±0.124	0.276±0.249	-2.160	0.049*	0.558
	ST	0.064±0.051	0.115±0.129	-1.420	0.178	0.367
	TA	0.745±0.210	0.811±0.125	-0.898	0.384	0.232
	GL	0.263±0.254	0.337±0.263	-0.693	0.500	0.179

Table 1. Muscle synergy analysis for 45° and 90° change of direction sprints. The table presents the mean and standard deviation (Mean±SD) of muscle activation levels for two different change of direction angles (45° and 90°) and their corresponding P values, effect sizes, and other data. * indicates $P < 0.05$; in the statistic column, ^a represents the z-value, while the others are t-values; in the effect size column, ^b represents the r-value, while the others are Cohen's d

Indicator	Synergy	45° (Mean±SD)	90° (Mean±SD)	Statistic	P-value	Effect size
Time to peak activation	Synergy 1	56.588±37.919	51.353±35.965	0.480	0.639	0.116
	Synergy 2	44.067±20.509	41.533±22.687	0.382	0.708	0.099
Activation level of synergy	Synergy 1	0.413±0.069	0.403±0.052	0.696	0.496	0.169
	Synergy 2	0.406±0.067	0.424±0.068	-0.867	0.400	0.224
Proportion of significant activation duration	Synergy 1	34.000±11.689	38.647±13.191	-1.523	0.147	0.369
	Synergy 2	36.267±14.295	36.067±13.414	-0.625 ^a	0.826	0.057 ^b
Overall synergy activation level	N/A	0.403±0.058	0.412±0.049	-0.832	0.418	0.208
Co-activation duration	N/A	5.750±6.137	5.688±6.041	0.026	0.980	0.007

Table 2. Differences in synergy parameters. This table outlines the differences in various synergy parameters for 45° and 90° change of direction sprints, including the mean and standard deviation (Mean±SD) of the parameters and their corresponding P values, effect sizes, and other data. N/A: Not applicable; in the statistic column, ^a represents the z-value, while the others are t-values; in the effect size column, ^b represents the r-value, while the others are Cohen's d

allocation for ankle joint control. Future research could integrate techniques such as electroencephalography (EEG) to further validate the adaptive mechanisms of neural control strategies.

The quadriceps serve as a key muscle group during the deceleration phase of COD maneuvers^{10,34}, with their neuromuscular control patterns demonstrating significant alterations as the COD angle increases. Havens et al.³⁵ found that the deceleration demands during 90° COD are not uniformly distributed across all joints, but rather place greater emphasis on the knee joint. During deceleration, the knee joint is subjected to increased shear forces and torsional moments, with anterior shear forces also rising correspondingly³⁶. Hader et al.¹⁰ further confirmed that the vastus lateralis exhibits greater muscular activity during sharper COD maneuvers. At 90° COD, generating greater lateral center of mass-center of pressure distance and subsequent lateral propulsion requires increased hip abduction^{35,37}, which redirects the force vector more laterally relative to the knee joint center^{35,38} and potentially elevates knee abduction moments. Based on this context, the current study proposes that the significant increase in the weighting of the vastus lateralis (VL) within Synergy Module 2 primarily serves a dual requirement for knee joint stability: it must enhance the knee extension moment to counteract greater centrifugal loads, while simultaneously modulating the abduction moment to balance the increased knee valgus tendency resulting from lateral displacement of the center of mass. However, the above interpretation still requires future validation through integration with actual biomechanical data (such as lower limb kinematics, kinetics, and joint moments).

Numerous training studies have demonstrated that enhancing hamstring strength can effectively improve COD performance^{39,40}. For example, Siddle et al.⁴¹ found that six weeks of Nordic hamstring curl (NHC) training simultaneously improved COD speed and reduced injury risk; Adıgüzel et al.⁴² also reported that an eight-week NHC program led to an 8% improvement in COD capacity. These long-term training benefits underscore the

fundamental role of the hamstrings in COD movements. The observed increase in biceps femoris (BF) activation during 90° COD in this study further confirms the central functional importance of the hamstrings: it indicates that the nervous system immediately upregulates hamstring recruitment when confronting greater deceleration loads and stability demands.

During the 90° COD test, the observed significant reduction in tibialis anterior (TA) weighting within Synergy Module 1⁴³ warrants attention. As a primary ankle dorsiflexor, diminished TA activation may compromise dynamic foot stability during the deceleration phase⁴³, consequently elevating the risk of ankle inversion injuries. Therefore, in COD training, it is necessary to specifically strengthen the control ability of the ankle joint in deceleration scenarios, such as combining dorsiflexion eccentric training with an unstable surface.

In the COD movement, athletes must rapidly decelerate their body's momentum after high-speed sprinting before promptly reaccelerating. In this process, the eccentric contraction capacity of synergistic muscle groups such as the hamstrings, gluteus maximus, and soleus becomes the fundamental guarantee for deceleration efficiency and knee joint stability⁴⁴. Among these, the hamstrings, as one of the core synergistic muscle groups, together with the gluteus maximus and soleus, form a mechanical buffer system that counteracts body inertia⁴⁴, with eccentric strength serving as the key factor ensuring both deceleration performance and knee stability.

From the perspective of neuromuscular control, the activation pattern of the hamstring muscles has a significant impact on knee joint stability. Studies have confirmed that the strength ratio of the hamstrings to the quadriceps is a core indicator for reducing the risk of secondary ACL injuries⁴⁵. When the knee joint approaches full extension, the shear force on the ACL reaches its peak, significantly increasing the risk of injury⁴⁶. The hamstrings can generate a posterior moment, which can create a mechanical balance with the quadriceps. This co-activation pattern helps maintain the dynamic stability of the knee joint⁴⁷. Therefore, in deceleration training, it is necessary to strengthen the co-working ability and eccentric contraction ability of the core muscle groups (hamstrings, quadriceps, etc.) in different angle COD scenarios (such as Nordic hamstring training⁴⁸), to meet the needs of turning.

Although this study initially revealed the impact of change-of-direction angles on the lower limb muscle coordination patterns during deceleration, several limitations still exist. First, the study only compared two change-of-direction angles, 45° and 90°, and did not cover other angles or more complex multi-gait cycle deceleration scenarios. Therefore, the generalizability of the conclusions needs further validation. Second, the sample size was limited (n=16), and the differences in neuromuscular control strategies among individuals may have had some impact on the stability of the overall results. In terms of statistical analysis, this study did not perform statistical correction for multiple comparisons. Although this was based on the exploratory nature of the study to avoid missing potentially meaningful findings due to excessive correction, it may have increased the risk of Type I errors (false positives). Therefore, the significant differences reported in the text (especially those with P values close to 0.05) should be regarded as preliminary evidence, and their robustness needs to be confirmed by subsequent larger-sample validation studies. In addition, regarding electromyography collection, this study only placed a single pair of electrodes in the middle segment of each muscle. Although this is in line with the conventional operation specifications of surface electromyography, it cannot reflect the functional zoning phenomena caused by differences in fiber orientation, activation timing, and motor unit recruitment strategies in the proximal and distal parts of the same muscle. In recent years, studies on muscle regional differences by Sahinis et al.⁴⁹ and on functional zoning of the semitendinosus muscle⁵⁰ have indicated that this spatial heterogeneity of muscles may affect the interpretation of muscle synergies. Therefore, single-point recording may underestimate the true neuromuscular control strategies. In future studies, it is necessary to use high-density surface EMG or multi-site synchronous acquisition technology to more comprehensively and accurately characterize the overall muscle synergy features⁵¹.

Conclusion

This study, through comparative analysis of the muscle synergy patterns during deceleration steps in 45° and 90° COD sprints, has revealed the adaptive regulatory mechanisms of the nervous system in response to different turning requirements. The findings are as follows: 1) In both COD angles, two stable muscle synergy modules were identified. Synergy 1 was dominated by the biceps femoris, semitendinosus, and vastus lateralis, while synergy 2 was centered on the rectus femoris, vastus medialis, and tibialis anterior. These modules collectively contribute to deceleration, initial direction change, and joint stability maintenance. 2) As the COD angle increased from 45° to 90°, the weight of the tibialis anterior (TA) in synergy module 1 significantly decreased, while the weights of the vastus lateralis (VL) and biceps femoris (BF) in synergy module 2 significantly increased. This change reflects that the nervous system, in response to the higher deceleration demands, strengthens knee joint stability while relatively reducing ankle joint control. 3) During 90° changes of direction, the risk of ACL injury increases and ankle joint stability decreases. Therefore, targeted training should focus on: optimizing knee joint stability; strengthening the eccentric power of the hamstrings; and enhancing dynamic control of the ankle joint.

Data availability

The results of this study have been deposited in the Figshare database. The website is: <https://doi.org/10.6084/m9.figshare.30092332.v1>

Received: 16 September 2025; Accepted: 3 December 2025

Published online: 16 December 2025

References

1. Barrera-Domínguez, F. J. et al. Strength characteristics in faster change of direction basketball players: A comparison across cutting angles. *Eur. J. Sport Sci.* **24**, 1260–1269 (2024).
2. Trajković, N., Sporiš, G., Kristićević, T., Madić, D. M. & Bogataj, Š. The importance of reactive agility tests in differentiating adolescent soccer players. *Int. J. Environ. Res. Public Health* **17**, 3839 (2020).
3. Gabbett, T. J. Physiological and anthropometric characteristics of starters and non-starters in junior rugby league players, aged 13–17 years. *J. Sports Med. Phys. Fit.* **49**, 233–239 (2009).
4. Spiteri, T., Cochrane, J. L., Hart, N. H., Haff, G. G. & Nimphius, S. Effect of strength on plant foot kinetics and kinematics during a change of direction task. *Eur. J. Sport Sci.* **13**, 646–652 (2013).
5. Jones, P., Thomas, C., Dos’Santos, T., McMahon, J. & Graham-Smith, P. The role of eccentric strength in 180° turns in female soccer players. *Sports* **5**, 42 (2017).
6. Dos’Santos, T., Thomas, C., Jones, P. A. & Comfort, P. Mechanical determinants of faster change of direction speed performance in male athletes. *J. Strength Cond. Res.* **31**, 696–705 (2017).
7. Dos’Santos, T., Thomas, C. & Jones, P. A. How early should you brake during a 180° turn? A kinetic comparison of the antepenultimate, penultimate, and final foot contacts during a 505 change of direction speed test. *J. Sports Sci.* **39**, 395–405 (2021).
8. Ade, J., Fitzpatrick, J. & Bradley, P. S. High-intensity efforts in elite soccer matches and associated movement patterns, technical skills and tactical actions. Information for position-specific training drills. *J. Sports Sci.* **34**, 2205–2214 (2016).
9. Harper, D. J., Carling, C. & Kiely, J. High-intensity acceleration and deceleration demands in elite team sports competitive match play: A systematic review and meta-analysis of observational studies. *Sports Med.* **49**, 1923–1947 (2019).
10. Hader, K., Mendez-Villanueva, A., Palazzi, D., Ahmadi, S. & Buchheit, M. Metabolic power requirement of change of direction speed in young soccer players: Not all is what it seems. *PLOS One* **11**, e0149839 (2016).
11. Falch, H. N., Reædergård, H. G. & Van Den Tillaar, R. Effect of approach distance and change of direction angles upon step and joint kinematics, peak muscle activation, and change of direction performance. *Front. Sports Act. Living* **2**, 594567 (2020).
12. Philipp, N. M. et al. Horizontal deceleration performance in professional female handball players. *Biomechanics* **3**, 299–309 (2023).
13. Harper, D. J. et al. Biomechanical and neuromuscular performance requirements of horizontal deceleration: A review with implications for random intermittent multi-directional sports. *Sports Med.* **52**, 2321–2354 (2022).
14. Pan, Z., Liu, L., Li, X. & Ma, Y. Characteristics of muscle synergy and anticipatory synergy adjustments strategy when cutting in different angles. *Gait Posture* **107**, 114–120 (2024).
15. Hagedoorn, L., Zadravec, M., Olenšek, A., Van Asseldonk, E. & Matjačić, Z. The existence of shared muscle synergies underlying perturbed and unperturbed gait depends on walking speed. *Appl. Sci.* **12**, 2135 (2022).
16. Del Vecchio, A. et al. The forces generated by agonist muscles during isometric contractions arise from motor unit synergies. *J. Neurosci.* **43**, 2860–2873 (2023).
17. Wojtara, T., Alnajjar, F., Shimoda, S. & Kimura, H. Muscle synergy stability and human balance maintenance. *J. NeuroEng. Rehabil.* **11**, 129 (2014).
18. Hermens, H. J., Freriks, B., Disselhorst-Klug, C. & Rau, G. Development of recommendations for SEMG sensors and sensor placement procedures. *J. Electromyogr. Kinesiol. Off. J. Int. Soc. Electrophysiol. Kinesiol.* **10**, 361–374 (2000).
19. Georgoulis, J. D. et al. Neuromuscular activity of the lower-extremities during running, landing and changing-of-direction movements in individuals with anterior cruciate ligament reconstruction: A review of electromyographic studies. *J. Exp. Orthop.* **10**, 43 (2023).
20. Kobsar, D., Osis, S. T., Phinyomark, A., Boyd, J. E. & Ferber, R. Reliability of gait analysis using wearable sensors in patients with knee osteoarthritis. *J. Biomech.* **49**, 3977–3982 (2016).
21. Schreurs, M. J. Sharper angle, higher risk? The effect of cutting angle on knee mechanics in invasion sport athletes. *J. Biomech.* (2017).
22. Hajiloo, B., Anbarian, M., Esmaeili, H. & Mirzapour, M. The effects of fatigue on synergy of selected lower limb muscles during running. *J. Biomech.* **103**, 109692 (2020).
23. Hanawa, H. et al. Muscle synergies underlying sit-to-stand tasks in elderly people and their relationship with kinetic characteristics. *J. Electromyogr. Kinesiol.* **37**, 15–20 (2017).
24. Lee, D. D. & Seung, H. S. Learning the parts of objects by non-negative matrix factorization. *Nature* **401**, 788–791 (1999).
25. Jeong, H. et al. Muscle coordination and recruitment during squat assistance using a robotic ankle–foot exoskeleton. *Sci. Rep.* **13**, 1363 (2023).
26. Li, S. et al. Evaluation of functional correlation of task-specific muscle synergies with motor performance in patients poststroke. *Front. Neurol.* **8**, 337 (2017).
27. Sawers, A., Allen, J. L. & Ting, L. H. Long-term training modifies the modular structure and organization of walking balance control. *J. Neurophysiol.* **114**, 3359–3373 (2015).
28. Kim, M., Kim, Y., Kim, H. & Yoon, B. Specific muscle synergies in national elite female ice hockey players in response to unexpected external perturbation. *J. Sports Sci.* **36**, 319–325 (2018).
29. Yokoyama, H., Ogawa, T., Kawashima, N., Shinya, M. & Nakazawa, K. Distinct sets of locomotor modules control the speed and modes of human locomotion. *Sci. Rep.* **6**, 36275 (2016).
30. Cappellini, G., Ivanenko, Y. P., Poppele, R. E. & Lacquaniti, F. Motor patterns in human walking and running. *J. Neurophysiol.* **95**, 3426–3437 (2006).
31. Saito, A., Tomita, A., Ando, R., Watanabe, K. & Akima, H. Muscle synergies are consistent across level and uphill treadmill running. *Sci. Rep.* **8**, 5979 (2018).
32. Smith, S., Allan, R., Marreiros, S., Woodburn, J. & Steultjens, M. Muscle co-activation across activities of daily living in individuals with knee osteoarthritis. *Arthritis Care Res.* **71**, 651–660 (2019).
33. Darainy, M. & Ostry, D. J. Muscle cocontraction following dynamics learning. *Exp. Brain Res.* **190**, 153–163 (2008).
34. Rand, M. K. & Ohtsuki, T. EMG analysis of lower limb muscles in humans during quick change in running directions. *Gait Posture* **12**, 169–183 (2000).
35. Havens, K. L. & Sigward, S. M. Joint and segmental mechanics differ between cutting maneuvers in skilled athletes. *Gait Posture* **41**, 33–38 (2015).
36. Myer, G., Ford, K. & Hewett, T. The effects of gender on quadriceps muscle activation strategies during a maneuver that mimics a high ACL injury risk position. *J. Electromyogr. Kinesiol.* **15**, 181–189 (2005).
37. Sigward, S. M., Cesar, G. M. & Havens, K. L. Predictors of frontal plane knee moments during side-step cutting to 45 and 110 degrees in men and women: Implications for anterior cruciate ligament injury. *Clin. J. Sport Med. Off. J. Can. Acad. Sport Med.* **25**, 529–534 (2015).
38. Jones, P. A., Herrington, L. C. & Graham-Smith, P. Technique determinants of knee joint loads during cutting in female soccer players. *Hum. Mov. Sci.* **42**, 203–211 (2015).
39. Crawford, S. K. et al. The effects of hip- vs. knee-dominant hamstring exercise on biceps femoris morphology, strength, and sprint performance: A randomized intervention trial protocol. *BMC Sports Sci. Med. Rehabil.* **15**, 72 (2023).
40. Koc, M. et al. Impact of nordic hamstring breaking point angle on football player performance. *PeerJ* **13**, e19275 (2025).
41. Siddle, J. et al. Acute adaptations and subsequent preservation of strength and speed measures following a nordic hamstring curl intervention: A randomised controlled trial. *J. Sports Sci.* **37**, 911–920 (2019).

42. Adiguzel, N. S. et al. The effect of the nordic hamstring curl training program on athletic performance in young football players. *Appl. Sci.* **14**, 10249 (2024).
43. Mitchell, A., Dyson, R., Hale, T. & Abraham, C. Biomechanics of ankle instability. Part 1: Reaction time to simulated ankle sprain. *Med. Sci. Sports Exerc.* **40**, 1515–1521 (2008).
44. Mateus, R. B., Ferrer-Roca, V., João, F. & Veloso, A. P. Muscle contributions to maximal single-leg forward braking and backward acceleration in elite athletes. *J. Biomech.* **112**, 110047 (2020).
45. Hogberg, J. et al. No association between hamstrings-to-quadriceps strength ratio and second ACL injuries after accounting for prognostic factors: A cohort study of 574 patients after ACL-reconstruction. *Sports Med. Open* **10**, 7 (2024).
46. Quatman, C. E. & Hewett, T. E. The anterior cruciate ligament injury controversy: Is valgus collapse a sex-specific mechanism? *Br. J. Sports Med.* **43**, 328–335 (2009).
47. Weinhandl, J. T. et al. Reduced hamstring strength increases anterior cruciate ligament loading during anticipated sidestep cutting. *Clin. Biomech.* **29**, 752–759 (2014).
48. Sahinis, C., Amiridis, I. G., Enoka, R. M. & Kellis, E. Differences in activation amplitude between semitendinosus and biceps femoris during hamstring exercises: A systematic and critical review with meta-analysis. *J. Sports Sci.* **43**, 1054–1069 (2025).
49. Sahinis, C., Amiridis, I. G. & Kellis, E. Neuromechanical basis of region-specific differences and their implications for sport performance and injury prevention: A narrative review. *Eur. J. Appl. Physiol.* <https://doi.org/10.1007/s00421-025-05889-w> (2025).
50. Sahinis, C. et al. Distinct neural drives along the semitendinosus muscle. *Med. Sci. Sports Exerc.* **56**, 2338–2348 (2024).
51. Sahinis, C., Amiridis, I. G., Farina, D., Enoka, R. M. & Kellis, E. Independent neural drives and distinct motor unit discharge characteristics in hamstring muscles during isometric knee flexion. *Eur. J. Appl. Physiol.* <https://doi.org/10.1007/s00421-025-0595-3> (2025).

Author contributions

Conceptualization: Hongxiang Zhang, Haoyang Wang. Methodology: Hongxiang Zhang, Haoyang Wang, Huan Long. Writing—Original draft: Hongxiang Zhang, Xinyu Zhang, Haoyang Wang. Writing—review and editing: Huan Long, Haoyang Wang.

Declarations

Competing interests

The authors declare no competing interests.

Additional information

Correspondence and requests for materials should be addressed to H.L.

Reprints and permissions information is available at www.nature.com/reprints.

Publisher's note Springer Nature remains neutral with regard to jurisdictional claims in published maps and institutional affiliations.

Open Access This article is licensed under a Creative Commons Attribution-NonCommercial-NoDerivatives 4.0 International License, which permits any non-commercial use, sharing, distribution and reproduction in any medium or format, as long as you give appropriate credit to the original author(s) and the source, provide a link to the Creative Commons licence, and indicate if you modified the licensed material. You do not have permission under this licence to share adapted material derived from this article or parts of it. The images or other third party material in this article are included in the article's Creative Commons licence, unless indicated otherwise in a credit line to the material. If material is not included in the article's Creative Commons licence and your intended use is not permitted by statutory regulation or exceeds the permitted use, you will need to obtain permission directly from the copyright holder. To view a copy of this licence, visit <http://creativecommons.org/licenses/by-nc-nd/4.0/>.

© The Author(s) 2025